



Inhibition of Chikungunya virus genome replication by targeting essential RNA structures within the virus genome

Oliver Prosser, Nicola J. Stonehouse, Andrew Tuplin*

School of Molecular and Cellular Biology, Faculty of Biological Sciences and Astbury Centre for Structural and Molecular Biology, University of Leeds, Leeds, LS2 9JT, UK

ABSTRACT

Chikungunya virus (CHIKV) is a pathogenic arbovirus spread by *Aedes* spp. mosquitoes. CHIKV has a wide global prevalence and represents a significant health burden in affected populations. Symptoms of CHIKV infection include fever, rashes and debilitating joint and muscle pain, which can persist for several months to years in some patients. To date, there remains no vaccine or specific antiviral therapy against this important human pathogen. Based on our previously published structural and phenotypic analysis of the 5' region of the CHIKV genome, we designed a panel of locked nucleic acid oligonucleotides to bind structured RNA replication elements within the virus genome, which are essential for efficient CHIKV replication. Using electromobility shift assays, we confirmed the relative binding efficiencies of each LNA to target CHIKV genomic RNA. We then went on to demonstrate, using both sub-genomic replicon and infectious virus systems, that targeting individual RNA replication elements inhibits CHIKV genome replication and production of infectious virus. Time course assays demonstrated that LNAs can access the CHIKV replication complex and virus genome, during active virus replication. For the first time, these findings show that functional RNA elements can be specifically targeted during the CHIKV lifecycle and consequently represent potential novel antiviral targets.

1. Introduction

Chikungunya virus (CHIKV) is a member of the *alphavirus* genus of the *Togaviridae* family and was first identified in the 1950s in Tanzania (Robinson, 1955). CHIKV is spread by *Aedes aegypti* and *Aedes albopictus* mosquitoes and has caused major outbreaks throughout Africa, Asia, the Americas and the Caribbean (Burt et al., 2017; Van Bortel et al., 2014; Weaver and Lecuit, 2015). Genetic adaptation of CHIKV to *Ae. albopictus* (Tssetsarkin et al., 2007), which breeds in more temperate climates compared with *Ae. aegypti*, has led to concern that CHIKV may expand its endemic host range to more temperate regions, such as southern and central Europe (Gould et al., 2010; Rezza et al., 2007) and central America (Kendrick et al., 2014). Following infection, CHIKV replicates in dermal fibroblasts and spreads via the blood stream to several tissues including the liver, joints and muscle (Schwartz and Albert, 2010). Chikungunya fever presents as an acute febrile illness associated with rash, high fever, myalgia and malaise, progressing to severe polyarthralgia/polyarthritis (Ganesan et al., 2017; Oviedo-Pastrana et al., 2017). In some cases, more severe symptoms can occur, including encephalitis and Guillain Barré syndrome (Burt et al., 2017; Lemant et al., 2008). High morbidity is associated with chronic incapacitating arthralgia, (potentially associated with ongoing replication within the joint tissue) which can persist for several years after the initial acute disease (Schilte et al., 2013). There are currently no specific antiviral

agents or vaccines available for CHIKV, making the development of novel, specific therapies a priority for research.

CHIKV is a small, enveloped virus with an 11.8 kb positive-sense RNA genome. The RNA genome consists of two open reading frames (ORFs), separated by a non-coding intergenic region and flanked by a 5' UTR of 76 nt and a 3' UTR of between 450 and 900 nucleotides in length (Dubey et al., 2019; Li et al., 2012; Solignat et al., 2009). The 5' UTR is capped with a type-0 cap structure (N7mGppp) for initiation of cap-dependent translation and the 3' end of the genome has a polyadenylate tail. ORF 1 encodes the non-structural proteins (nsp1-4), which form the components of the replication complex (Mathur et al., 2016; Strauss and Strauss, 1994), the most highly conserved of which is the RNA-dependent RNA polymerase (RdRp) nsp4 (Pietilä et al., 2017b). During CHIKV replication, the ORF 1 encoded viral polyprotein P1234 is proteolytically cleaved in *cis* by nsp2, releasing nsp4 and initiating minus-strand RNA synthesis. Proteolytic cleavage of the P123 polyprotein initiates synthesis of the positive-stranded genomic and sub-genomic RNAs from the minus-strand template. The structural proteins (C, E3, E2, E1 and 6K) are translated from ORF-2 26S sub-genomic RNAs (Gebhart et al., 2015) and are involved in cell entry and formation of progeny virus particles (Mathur et al., 2016). CHIKV RNA replication occurs in membrane bound spherules derived from plasma membrane, which have been proposed to act as scaffolds for replication complexes and provide protection from cytosolic pattern

* Corresponding author.

E-mail address: A.K.Tuplin@leeds.ac.uk (A. Tuplin).

<https://doi.org/10.1016/j.antiviral.2023.105523>

Received 29 September 2022; Received in revised form 22 December 2022; Accepted 2 January 2023

Available online 2 January 2023

0166-3542/© 2023 The Authors. Published by Elsevier B.V. This is an open access article under the CC BY license (<http://creativecommons.org/licenses/by/4.0/>).

recognition receptors (Gebhart et al., 2015; Thaa et al., 2015).

Using a combination of Selective 2' Hydroxyl Acylation analysed by Primer Extension (SHAPE) constrained thermodynamic modelling and structure based reverse genetics approaches, we previously characterised RNA structural elements (RREs) within the first 300 nt of the CHIKV genome, demonstrating that these structures are essential for efficient virus genome replication (Fig. 1) (Kendall et al., 2019). Two RNA replication elements (SL3 and SL47) were identified within the 5' UTR and five in the adjacent nsp1 encoding region of ORF1 (SL85, SL102, SL165, SL194 and SL246). SL3 is required for genome replication in both human and mosquito cells. By contrast, SL47, SL85, SL102, SL165 and SL194 are only required in human cells, whilst SL246 is only required in mosquito cells (Kendall et al., 2019). SL165 and SL194 correspond to the 51 nt nsp1 conserved sequence element (CSE), which is highly conserved in structure and sequence across the alphavirus genus (Fayzulin and Frolov, 2004; Frolov et al., 2001; Kulasegaran-Shylini et al., 2009; Niesters and Strauss, 1990). In CHIKV, the 51 nt element enhanced replication in human cells but does not have significant effect on virus replication in *Ae. albopictus* derived cells - in contrast to VEEV and SINV where the 51 nt element enhances replication in both vertebrate and invertebrate derived cells. Reverse genetic studies demonstrated that SL165 functions through a structure dependent and sequence independent mechanism. In contrast, the function of SL194 was dependent on both the primary sequence of its terminal unpaired loop and the structure of the heteroduplex stem, with the terminal loop acting as a CHIKV-specific signal motif (Kendall et al., 2019).

Locked nucleic acids (LNA) are oligonucleotides which contain one or more modified nucleotide bases, in which the ribose moiety has been locked in a single conformational state (Grünweller and Hartmann, 2007; Suresh and Priyakumar, 2013). LNA bases can be incorporated into DNA oligonucleotides - which exhibit increased melting temperature, specificity and nuclease resistance. Spacing of LNA nucleotides within the sequence, such that there are no more than four consecutive DNA bases, provides resistance to RNase H cleavage of DNA/RNA hybrids (Kurreck et al., 2002).

Viral RNA structures have previously been targeted using a variety of methods. (Marton et al., 2012; Tuplin et al., 2015). Antisense LNA oligonucleotides (hereafter referred to as LNAs) have been shown to inhibit

translation of sequences encoding VP24 and the nucleoprotein of Ebola virus (Chery et al., 2018), to interfere with HIV-1 genome dimerization (Elmén et al., 2004) and to disrupt a conserved RNA structure in hepatitis C virus (Tuplin et al., 2015). Miravirsin, an LNA inhibitor targeting host miR-122 reached phase 2 clinical trials for treatment of HCV (Gebert et al., 2014; Titze-de-Almeida et al., 2017). Using our detailed structural and function knowledge of the CHIKV 5' genome region, we designed antisense LNAs to target SL165, SL194 and the stem region upstream of SL194 - with the aim of inhibiting virus replication by disrupting both RNA-RNA and RNA-protein interactions, essential for CHIKV genome replication. Using infectious virus and sub-genomic replicon systems, for the first time we demonstrate that an LNA targeting conserved RNA replication element SL165 inhibits CHIKV genome replication and subsequent production of infectious virus. Demonstrating that targeting RNA replication elements within the virus genome is a viable approach for both for the development of antiviral agents and research tools to further study CHIKV biology and the essential role of RNA replication elements.

2. Materials and methods

2.1. Cell culture

Huh7 and BHK-21 cells were a gift from Prof Harris (University of Leeds, UK). All cell lines tested negative for mycoplasma. Cells were maintained in Dulbecco's modified minimal essential medium (DMEM, Sigma) supplemented with 10% (v/v) FBS (Thermo Fisher Scientific), 100 units/ml penicillin, 100 µg/ml streptomycin and 0.1 mM non-essential amino acids (Lonza) and maintained at 37 °C in 5% CO₂.

2.2. DNA constructs

The infectious CHIKV (ICRES), CHIKV-Firefly luciferase sub-genomic replicon (Fluc-SGR) and CHIKV-translation reporter Fluc-Rluc-(GDD > GAA)-SGR cDNA clones were based on the ESCA strain, isolate LR2006 OPY1 (Pohjala et al., 2011). In Fluc-SGR, the second ORF was replaced by a firefly luciferase reporter gene. The Fluc-Rluc-(GDD > GAA)-SGR additionally had a *Renilla* luciferase gene fused within nsp3 and a GDD

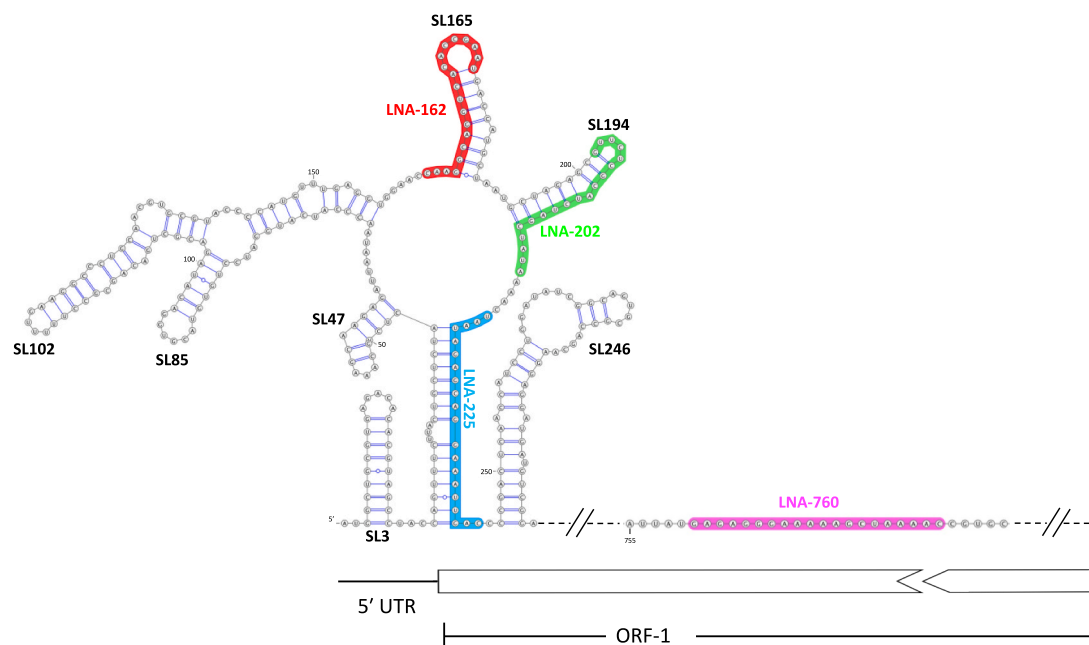


Fig. 1. Schematic representation of CHIKV RNA structures within the 5'UTR and adjacent ORF-1 region of the CHIKV genome (Kendall et al., 2019). RNA replication elements SL3, SL47, SL85, SL102, SL165, SL194 and SL246 are labelled in black type. The binding positions of antisense LNA-162 (Red), LNA-202 (Green), LNA-225 (Blue) and LNA-760 (Pink) are indicated by coloured shading.

> GAA mutation in nsp4 to block RdRp activity. A wild-type version of Fluc-Rluc-(GDD > GAA)-SGR was included as a control. Transfection control RNA (T7_Ren) encodes *Renilla* luciferase. Plasmid cDNA was purified using GeneJET Plasmid Maxiprep kits (Thermo Fisher Scientific) according to the manufacturer's instructions.

2.3. CHIKV 1–337 PCR reactions

PCR amplification was performed to generate DNA fragments encompassing the CHIKV 5' UTR and upstream region of ORF-1 (CHIKV 1–337). Reactions contained 100 ng of ICRES cDNA, 0.5 nM primers (For primer: TAATACGACTCACTATAGGGATGGCTGCGTGAGACACACG, Rev primer: CGCACTGCGCATCGGGCAGA), 1 μ M dNTPs, 1 x GC buffer (NEB), 2 U of Phusion DNA polymerase (NEB) and nuclease free water to a final volume of 50 μ l. The following cycling conditions were used: 1 x 95 °C for 2 min, 25 X (95 °C for 15s, 50 °C for 15s, 72 °C for 15s) and 1 x 72 °C for 5 min. PCR products were purified using a Wizard® SV Gel and PCR Clean-Up System (Promega) according to the manufacturer's instructions.

2.4. In vitro RNA transcription

To generate Fluc-SGR, Fluc-Rluc-(GDD > GAA)-SGR and infectious CHIKV RNA, 1 μ g of ICRES cDNA was linearised with Not-I HF and used as a template for transcription of 5' [m7G(5')ppp(5')G] capped (m7G capped) RNA, using an SP6 mMessage mMachine kit, according to the manufacturer's instructions (Life Technologies). Uncapped CHIKV 1–337 RNA, used 1 μ g of CHIKV 1–337 PCR DNA as a template for *in vitro* transcription using the SP6-Scribe™ standard RNA IVT kit, according to the manufacturer's instructions (Lucigen). For T7_Ren RNA, 1 μ g of DNA was linearised using XhoI, combined with 1 X RNAPol Reaction Buffer (NEB), supplemented with 4 mM each of ATP, UTP, CTP and GTP, 3 mM cap analogue, 14 mM MgCl₂, 0.32 units of Pyrophosphatase, Inorganic (yeast) (NEB), 160 units of RNase inhibitor (Promega) and 200 units of T7 polymerase. Reactions were incubated at 37 °C for 3 h. In all cases, following DNase I treatment, RNA was purified by LiCl precipitation and analysed by denaturing agarose gel electrophoresis.

2.5. ³²P end labelling

LNA oligonucleotides were 5' end labelled using ATP(γ -³²P). 60 pmol of LNA was combined with 2 μ l 10 x T4 Polynucleotide Kinase buffer (NEB), 3 μ l ATP(γ -³²P) 10 mCi/ml, 1 μ l T4 Polynucleotide Kinase (NEB) and nuclease free H₂O to a final volume of 20 μ l, incubated at 37 °C for 30 min followed by 65 °C for 20 min. LNAs were purified by ethanol precipitation and resuspended in 60 μ l 0.5 x TE buffer. For end labelling of CHIKV RNA, reactions were performed as above using 20 pmol of RNA and 1 μ l ATP(γ -³²P) 10 mCi/ml.

2.6. Electromobility shift assays

Electromobility shift assays (EMSAs) were performed using 3.125 pmol of CHIKV 1–337 RNA in 0.5 x TE buffer. RNA was incubated at 95 °C for 2 min and on ice for 2 min before 3.3 x RNA folding buffer (100 mM HEPES pH 8.0, 100 mM NaCl and 10 mM MgCl₂) was added to a final volume of 10 μ l and incubated for 20 min at 37 °C. 1.25 pmol of ³²P labelled LNAs was added and incubated at 37 °C for 30 min. Samples were combined with native loading buffer and analysed by 8% native PAGE. Following drying, gels were exposed to a phosphor screen and analysed using an FLA-5000 phosphorimager illumination laser 635 (Fujifilm). LNA binding efficiencies were quantified by densitometry, as a percentage of total lane density normalised to the corresponding negative control lane.

2.7. Virus production

1.2 x 10⁶ BHK cells were trypsinised and resuspended in 400 μ l ice-cold DEPC-PBS. Cells were then electroporated with 1 μ g 5'-capped CHIKV ICRES RNA in a 4 mm electrocuvette, with a single square wave pulse at 260 V for 25 ms using a Bio-Rad electroporator, before seeding into a T175 flask in 20 ml DMEM. After 24 h, supernatant was aspirated and titred by plaque assay on BHK cells.

2.8. CHIKV quantification by plaque assay

BHK cells were seeded at 1 x 10⁵ cells per well in 12-well plates and maintained overnight in 1 ml DMEM. The following day monolayers were washed with PBS and infected with 10-fold serial dilutions of CHIKV infection supernatant and incubated at 37 °C. 1 h.p.i monolayers were washed with PBS and covered with a 0.8% methylcellulose DMEM P/S overlay. Following a 48-h incubation, monolayers were fixed and stained (5% paraformaldehyde and 0.25% crystal violet respectively) before plaques were counted and virus titres expressed in plaque-forming units per ml (PFU/ml).

2.9. LNA cell viability assay

Huh7 cells were seeded in 96 well plates at 1 x 10⁴ cells per well and maintained overnight in 100 μ l of DMEM. The following day, monolayers were washed once with 1 x PBS and 25 μ l of opti-Mem reduced-serum media added. Transfection media was prepared according to the manufacturer's instructions using 0.2 μ l of Lipofectamine-2000 (Invitrogen) and made up to 25 μ l using opti-Mem. Where appropriate, LNAs were added to the transfection media in concentrations ranging from 10 nM to 10 μ M. 25 μ l of transfection media was added to the monolayers which were then maintained for 6-h before the media was removed and replaced with 100 μ l of 1 mg/ml Thiazolyl Blue Tetrazolium Bromide (MTT) (Sigma) and incubated at 37 °C in 5% CO₂ for 30 min. After incubation, MTT solution was replaced with 100 μ l DMSO and the plate shaken at 60 rpm for 5 min. Absorbance at 570 nm was determined using an Infinite F50 microplate reader (Tecan) and expressed as a percentage of untreated control cells (Supplementary Fig. 1).

2.10. LNA transfection of CHIKV infected cells

Huh7 cells were seeded in 12 well plates at a confluency of 1 x 10⁵ cells per well and maintained overnight. The following day, monolayers were infected with CHIKV (MOI 1) and incubated in 1 ml of DMEM for 3 h. Transfection media was prepared according to the manufacturer's instructions, using 2 μ l of Lipofectamine (2000) (Invitrogen) per well, an LNA concentration of 600 nM and a total volume of 200 μ l opti-Mem per well. Following a 3-h incubation, monolayers were washed with 1 x PBS before adding 800 μ l of opti-Mem and LNA transfection mix. Monolayers were then incubated for 4 h before washing with 1 x PBS and maintaining in 1 ml DMEM until time points were taken.

2.11. Dose response and time course assays for LNAs with infectious CHIKV

Huh7 cells were seeded in 12 well plates at a confluency of 1 x 10⁵ cells per well overnight in 1 ml of DMEM. The following day, monolayers were infected with CHIKV (MOI 1) and incubated in 1 ml of DMEM for 3 h. After washing with 1 X PBS the monolayers were transfected as described earlier. For time point assays, at appropriate h.p.i 250 μ l of supernatant was harvested, stored at -80 °C and replaced with 250 μ l DMEM. Released CHIKV titre for each time point was quantified by plaque assay.

2.12. Infection of LNA transfected Huh7 cells with CHIKV

Huh7 cells were seeded in 12 well plates at a confluency of 1×10^5 cells per well overnight in 1 ml of DMEM. The following day the monolayers were transfected with LNAs, as previously described. 4 h.p.t monolayers were washed with 1 x PBS and infected with CHIKV (MOI 10). 24 h.p.i. supernatant was harvested, stored at -80°C and CHIKV titre quantified by plaque assay.

2.13. Quantification of CHIKV Genome copies using qRT-PCR

Following infection and harvest of supernatant, monolayers were washed with 1 x PBS and lysed using 500 μl TRI Reagent® Solution (Applied Biosystems) following the manufacturer's instructions. RNA was resuspended in 20 μl of nuclease free water and quantified using a nanoDrop 1000 spectrophotometer (Thermo scientific). 1 μg of extracted RNA was used to generate cDNA using an RNA-to-cDNA kit (Applied Biosystems) according to the manufacturer's instructions.

Quantitative PCR was performed using the qPCR BIO SyGreen Blue Mix Lo-ROX (PCR Biosystems), with primers amplifying a 131 nt region of the CHIKV E1 sequence (Fwd primer: 5' GCATCAGC-TAAGCTCCGCGTC 3', Rev primer: 5' GGTGTCCAGGCTGAAGACATTG 3') (Pongsiri et al., 2012), 100 ng of cDNA template and the following cycling conditions: 95°C for 2 min, 40 x (95°C for 5 s, 60°C for 30 s), dissociation curve $60\text{--}95^\circ\text{C}$, as pre-defined by the Mx3005P thermal cycler (Agilent Technologies). For standards, to quantify copy numbers in the respective samples, *in vitro* transcribed CHIKV ICRES RNA was reverse transcribed and 10-fold serial dilutions from 10^{-2} to 10^{-7} used.

2.14. Assessment of CHIKV protein expression by western blot

Following infection and incubation, monolayers were lysed in IP lysis buffer and incubated at room temperature for 30 min. Protein levels were quantified using a Pierce™ BCA Protein Assay Kit (Thermo scientific) according to the manufacturer's instructions. Equal amounts of protein lysate were analysed by SDS-PAGE gel electrophoresis. Protein was transferred onto an Immobilon-FL PVDF transfer membrane (MERCCK) using a TE77X semi-dry transfer (Hoefer) at 15 V for 60 min. Membranes were blocked using diluted Odyssey® Blocking Buffer in PBS (LI-COR) for 30 min and probed with primary anti-capsid (1:1000, rabbit polyclonal, in-house) or anti-nsP1 (1:1000, rabbit polyclonal, in-house) (Tamberg et al., 2007) antibody, in addition to host cell protein actin (clone AC-15, mouse monoclonal, Sigma) in diluted Odyssey® Blocking Buffer in PBS (LI-COR) overnight at 4°C . The following morning, primary antibody was removed and membranes washed 3 times using PBS. Membranes were stained with secondary antibodies (IRDye® 800CW Donkey anti-Mouse; IRDye® 680LT Donkey anti-Rabbit; Li-Cor) for 1 h at room temperature, washed 3 times using 1 x PBS, dried and then imaged using an Odyssey® Fc Imaging System (Li-Cor).

2.15. Sub-genomic replicon assays

Huh7 cells were seeded in 24 well plates at 5×10^4 cells per well and maintained overnight. For dose response assays, monolayers were washed once in PBS before addition of 400 μl opti-Mem reduced-serum media and 100 μl transfection media. Transfection media was prepared according to the manufacturer's instructions, using 1 μl Lipofectamine 2000 (Invitrogen), 250 ng of sub-genomic replicon reporter RNA, 50 ng *Renilla* luciferase RNA, and appropriate concentrations of LNA, before being made up to 100 μl using opti-Mem. Monolayers were maintained for 6 h.p.t before being washed in PBS and lysed in 100 μl 1 x passive lysis buffer (Promega). Lysates were stored at -80°C , prior to analysis using Dual-luciferase substrate (Promega) in a FLUOstar Optima luminometer (BMG labtech). For the translation assays a similar protocol was followed except that 500 ng of Fluc-SGR or Fluc-Rluc-(GDD >

GAA)-SGR RNA was transfected.

2.16. CHIKV Translation assay

Huh7 cells were seeded at 5×10^4 cells per well in a 24 well plate and maintained overnight. Transfection media was prepared according to the manufacturer's instructions. 500 ng of Fluc-SGR or Fluc-Rluc-(GDD > GAA)-SGR RNA was combined with 1 μl lipofectamine 2000 (Invitrogen) and 100 μl opti-Mem per well. For LNA transfected wells, LNA was added to the RNA mix prior to the addition of lipofectamine 2000. Monolayers were washed once in PBS before addition of 400 μl opti-Mem reduced-serum media and 100 μl transfection media. At 4 h.p.t, monolayers were washed with PBS and 1 ml of DMEM was added. Monolayers were maintained until 4, 6 and 12 h.p.t, before washing with PBS and lysis with 100 μl passive lysis buffer 2.0 (Biotium). Lysates were stored at -80°C , prior to analysis using Dual-luciferase substrate (Promega) and a FLUOstar Optima luminometer (BMG labtech).

3. Results

We previously published a SHAPE constrained RNA structure map of the CHIKV 5' UTR and adjacent upstream ORF-1 encoding region. Using minimisation of folding free energy, phylogenetic analysis, RNA SHAPE reactivity and a range of reverse genetic approaches, we demonstrated that a number of RREs within this region of the CHIKV genome are essential for virus genome replication in both human and mosquito cells (Kendall et al., 2019). In the current study we investigated whether such structured RREs can be specifically targeted, in order to inhibit CHIKV replication. Based on our previously published RNA structure map, anti-sense LNAs were designed to specifically anneal to RREs within the 5' region of the CHIKV genome – with the intention of blocking formation of these essential elements and their interaction with *trans*-activating factors.

3.1. LNA design

We designed LNAs to target RREs SL165 (LNA-162) and SL194 (LNA-202) within the nsP1 encoding region of the CHIKV genome (Fig. 1 and Supporting Fig. 1) (Kendall et al., 2019). Two negative control LNAs were also designed to anneal within the nsP1 encoding regions. The first negative control LNA (LNA-225) targeted a structured region of the genome downstream of SL194 and the second (LNA-760) targeted a downstream unstructured region of the virus genome (Fig. 1 and Supporting Fig. 1). A negative control scrambled-LNA was also designed, which had a similar base composition to the other LNAs but was not predicted to anneal to the CHIKV genome. To ensure high affinity binding and specificity, all LNAs were designed to form complete duplexes with an RNA hybridisation T_m of $\geq 80^\circ\text{C}$. BLASTn analysis with default settings against human and CHIKV genomes also confirmed that there were no predicted interactions with other regions of the virus or human genome. Qiagen (formerly Exiqon) LNA T_m Oligo design tools and guidelines were used in order to minimise LNA oligonucleotide secondary structure or self-complementarity.

3.2. Evaluation of LNA binding

In order to confirm LNA hybridisation to the CHIKV genome, electrophoretic mobility shift assays (EMSA) were performed (Fig. 2). The ability of ^{32}P 5' end labelled LNAs to anneal to unlabelled folded *in vitro* transcribed CHIKV RNA molecules (CHIKV 1–337) was assayed by EMSA, using native PAGE analysed by phosphorimaging. RNA/LNA- ^{32}P complexes were expected to migrate as larger molecules relative to unbound LNA- ^{32}P . The relative position of the LNA/RNA complexes was confirmed by comparison to unbound radiolabelled CHIKV 1–337 RNA and band shift analysis. Comparing equimolar amounts of bound and unbound LNA- ^{32}P , enabled comparative quantification of LNA-RNA

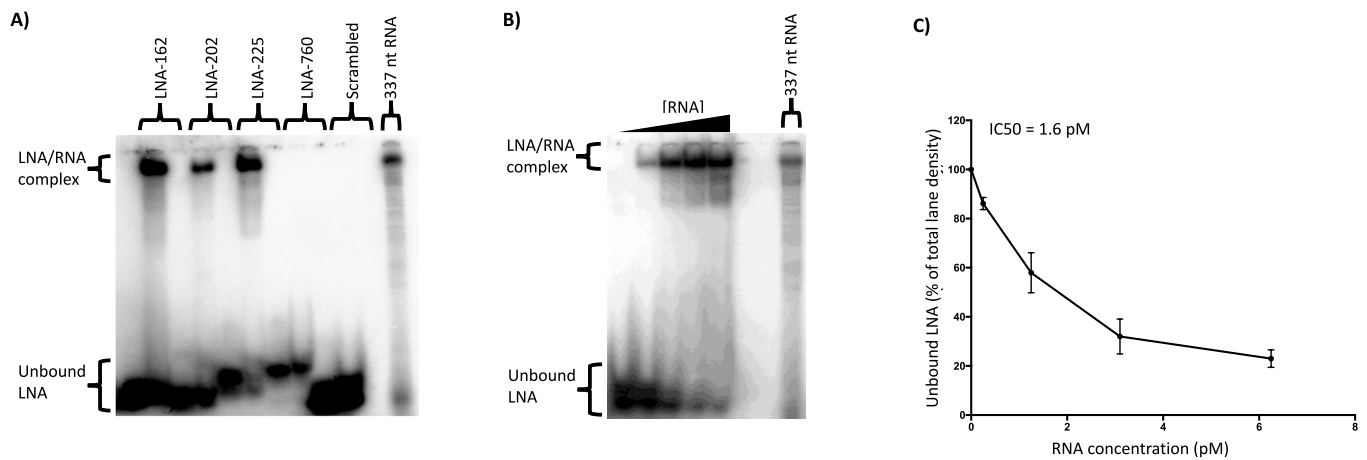


Fig. 2. LNA/RNA EMSA binding analysis for CHIKV RNA nts 1–336 **A)** LNA-162, LNA-202, LNA-225, LNA-760 and scrambled LNA were 5' radiolabelled prior to incubation with unlabelled folded CHIKV 1–337 RNA. 5' radiolabelled 1–337 CHIKV RNA without LNA was analysed in parallel and unbound LNA and LNA/RNA complexes are indicated. **B)** 32P labelled LNA-162 was incubated with increasing concentrations of unlabelled folded CHIKV 1–337 RNA. 5' radiolabelled 1–337 CHIKV RNA without LNA was analysed in parallel and unbound LNA and LNA/RNA complexes are indicated. **C)** Binding efficiency for LNA-162 was quantified using densitometry and expressed as percentage of unbound LNA-162 relative to total lane density. N = 3, error bars represent standard error from the mean.

target annealing.

EMSA confirmed that LNA-165, LNA-202 and LNA-225 were able to hybridise to CHIKV 1–337 RNA, confirming that their primary sequence motif target sequences were accessible for hybridisation, in the context of the folded RNA molecule (Fig. 2A). As predicted, control LNA-760 and scrambled-LNA did not hybridise to CHIKV 1–337 RNA bait. Of the two CHIKV RRE specific LNAs, LNA-162 demonstrated the greatest level of binding and was therefore taken forward for more detailed analysis. In order to further investigate LNA-162/CHIKV 1–337 binding kinetics, EMSA analysis was conducted in which a fixed excess concentration of LNA-162-³²P was titrated against increasing concentrations of CHIKV 1–337 target RNA (Fig. 2 B and C). These results confirmed a dose response towards RNA/LNA³²P complex formation, which following quantification by densitometric analysis indicated an IC₅₀ of 1.6 pM.

3.3. LNA-162 inhibits CHIKV replication

LNA-162 was designed to hybridise to RRE SL165, which is essential for efficient virus genome replication. Consequently, following confirmation of LNA-162/CHIKV RNA hybridisation, we wanted to investigate the effect of LNA-162 on CHIKV replication. Huh7 cells were infected with CHIKV and incubated for 3 h to allow formation of membrane bound replication complexes (Pietilä et al., 2017a), which are the site of CHIKV genome replication. Infected cells were then transfected with 600 nM LNAs and incubated for a further 21 h. Following this, supernatant was harvested and infectious released virus quantified by plaque assay in order to measure productive CHIKV replication (Fig. 3A). Relative to the scrambled-LNA transfected control, cells transfected with LNA-162 showed 80% inhibition in productive virus replication. By comparison, transfection with negative control LNAs LNA-225 and

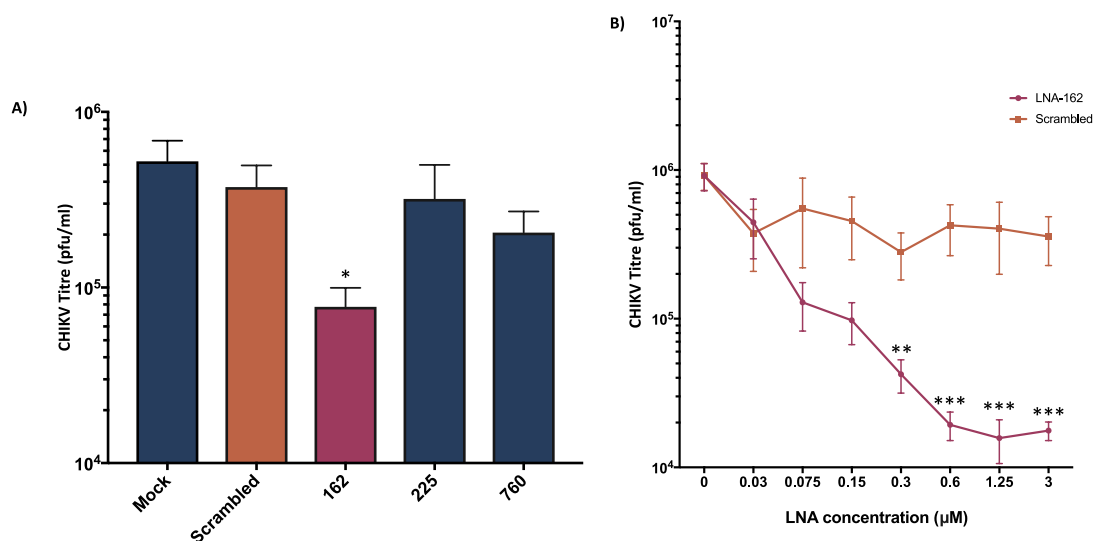


Fig. 3. LNA-162 transfection into Huh7 cells inhibited productive CHIKV replication with a positive dose response to increasing LNA-162 concentrations. **A)** Analysis of productive CHIKV replication following transfection of 600 nM LNA-162, LNA-225, LNA-760 and scrambled LNA into Huh7 cells 3 hpi at an MOI of 1. **B)** Dose response analysis of productive CHIKV replication following transfection of increasing concentrations of LNA-162 and scrambled LNA (0, 0.03, 0.075, 0.15, 0.3, 0.6, 1.25 and 3 µM) into Huh7 cells 3 hpi at an MOI of 1. Productive CHIKV replication measured at 24 hpi. N = 3, error bars represent standard error from the mean and significance was measured by two-tailed T-test for LNA-162 vs scrambled LNA (* = P < 0.05, ** = P < 0.01, *** = P < 0.001).

LNA-760 had no significant effect on CHIKV productive replication.

Having demonstrated that LNA-162 was able to inhibit CHIKV replication, we next confirmed the effect of a range of LNA concentrations on CHIKV replication in a dose response assay (Fig. 3B). Huh7 cells were infected with CHIKV, incubated for 3 h and then transfected with increasing concentrations of either LNA-162 or a non-specific scrambled-LNA control. Relative to the scrambled control, concentrations of LNA-162 ≥ 300 nM demonstrated significant inhibition of CHIKV replication in a dose dependent manner.

LNA-162 inhibition of CHIKV replication was further confirmed by western blot comparison of virus capsid protein expression in cells transfected with LNA-162, scrambled-LNA or a mock transfection control (Fig. 4A). As previously described, cells were transfected at 3 h post infection (h.p.i.) and harvested at 24 h.p.i. Monolayers transfected with LNA-162 had reduced expression of capsid protein compared with the mock transfection control and scrambled-LNA transfected cells. In a complimentary alternative approach qRT-PCR was also used to confirm significant inhibition of CHIKV replication. Following LNA-162 transfection 3 h.p.i with CHIKV an $\sim 80\%$ reduction in CHIKV genome copies relative to the scrambled -LNA control was observed (Fig. 4B).

We next investigated the effects if LNA-162 at different time points post LNA transfection (Fig. 5A). Huh7 cells were infected with CHIKV and transfected with LNA-162 or scrambled-LNA 3 h.p.i. CHIKV was harvested at 7, 12, 16, 24 and 48 h.p.i and titres of released virus determined by plaque assay (Fig. 5A). At all-time points measured LNA-162 significantly inhibited productive CHIKV replication, relative to the scrambled-LNA control. At 7, 12, 16 and 24 h.p.i LNA-162 inhibited CHIKV replication by between 70 and 89% - peaking at 89% inhibition at 16 h.p.i. By 48 h.p.i., inhibition was reduced to $\sim 80\%$.

To investigate if LNA-165 would have an increased or diminished effect on CHIKV replication if present in the cellular environment prior to productive infection, inhibition of virus replication was measured in Huh7 cells transfected with LNAs prior to virus infection (Fig. 5B). Here cells were transfected with LNA-162, scrambled-LNA or mock transfected and incubated for 4 h prior to infection. CHIKV was harvested at 24 h.p.i. and virus titre measured by plaque assay on BHK cells (Fig. 4B). Interestingly, very similar levels of inhibition were observed ($>85\%$ compared to scrambled-LNA) as for previous assays, in which the LNAs were transfected after infection.

3.4. LNA-162 Inhibits CHIKV genome replication

In order to confirm which stage of the virus lifecycle was being impaired by LNA-162, we used a CHIKV sub-genomic replicon system (CHIKV SGR). The CHIKV-SGR expresses the non-structural CHIKV proteins (nsp1-4) from ORF-1 but expresses a firefly luciferase reporter

from the second ORF - in place of the viral structural protein encoding genes (Fig. 6). Since the sub-genomic replicon encodes all the ORF-1 CHIKV non-structural proteins this system can be used to investigate viral genome replication in isolation from entry, packaging and egress events.

The effect of LNA-162 on CHIKV-SGR replication was measured in Huh7 cells at 6 h post-co-transfection with LNAs, CHIKV-SGR and a 5' capped *Renilla* luciferase RNA as a transfection control. Cells were transfected with LNAs at a range of concentrations, from 20 nM to 250 nM, in order to investigate dose dependent effects on CHIKV genome replication (Fig. 7A and Supplementary Fig. 3). At the lowest LNA concentration of 20 nM LNA-162 did not have a significant effect on replicon replication. However, the CHIKV-SGR was significantly inhibited by LNA-162 concentrations above 30 nM, with a maximum inhibition of 99% relative to the scrambled-LNA control at 250 nM. Levels of CHIKV-SGR replication may be affected at the levels of both genome replication and ORF-1 replicase protein translation. In order to investigate translation, in isolation from genome replication, we used a replication-deficient sub-genomic replicon (Fluc-Rluc-(GDD > GAA)-SGR), in which ORF-1 translation from input RNA could be measured by expression of a *Renilla* luciferase gene fused within nsP3 (Fig. 6C). Following co-transfection of Fluc-Rluc-(GDD > GAA)-SGR with either LNA-162, scrambled-LNA or a no LNA negative control, *Renilla* luciferase expression was measured 6 h post transfection. No significant inhibition of *Renilla* expression was observed (Fig. 7B). Taken together with our previous results demonstrating LNA-162 inhibition of CHIKV-SGR replication, these results are consistent with LNA-162 inhibiting CHIKV replication at the level of genome replication, rather than translation.

4. Discussion

In this study, for the first time we demonstrate that CHIKV replication can be inhibited by disruption of genome replication through targeting an essential RRE within the virus genome. We show that an LNA specific to RRE SL165 can inhibit CHIKV genome replication, presumably by disrupting the essential folding conformation of the stem-loop structure or via disruption of essential *trans* activating RNA binding proteins. We therefore demonstrate the principle that essential RNA structures within the CHIKV genome may represent novel antiviral targets. Our previous studies have demonstrated that six RREs within the 5' UTR and adjacent ORF-1 region of the CHIKV genome are essential to viral genome replication in human and mosquito cells (Kendall et al., 2019). Reverse genetic analysis demonstrated that each of these RNA elements is essential for efficient CHIKV genome replication and functions in a structure dependent manner. In the current study we

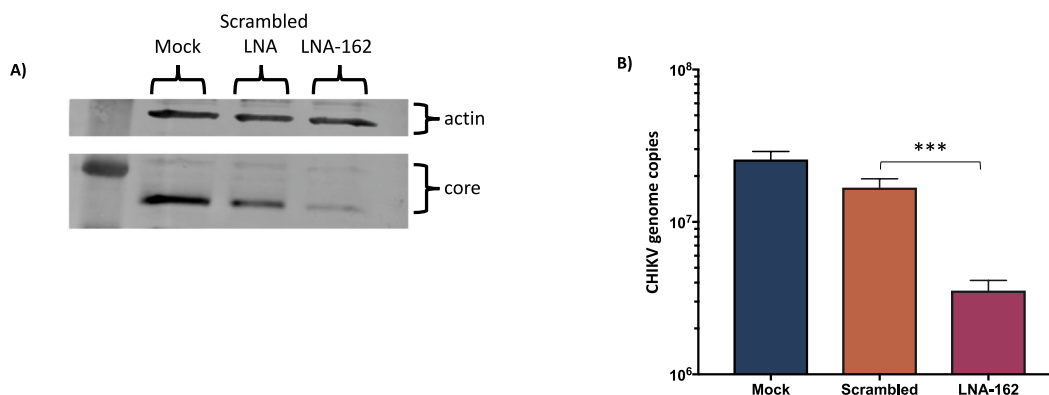


Fig. 4. LNA-162 transfection at 3 hpi (MOI: 1) into Huh7 cells inhibited CHIKV replication when measured by western blot and qRT-PCR. **A)** Intracellular expression levels of CHIKV C protein were determined by western blot at 24 hpi and compared between LNA-162, LNA-scrambled or a mock transfection control. **B)** Genomic positive strand CHIKV RNA copy number was determined by qRT-PCR. N = 3, error bars represent standard error from the mean and significance was measured by two-tailed T-test for LNA-162 vs scrambled LNA (* = $P < 0.05$, ** = $P < 0.01$, *** = $P < 0.001$).

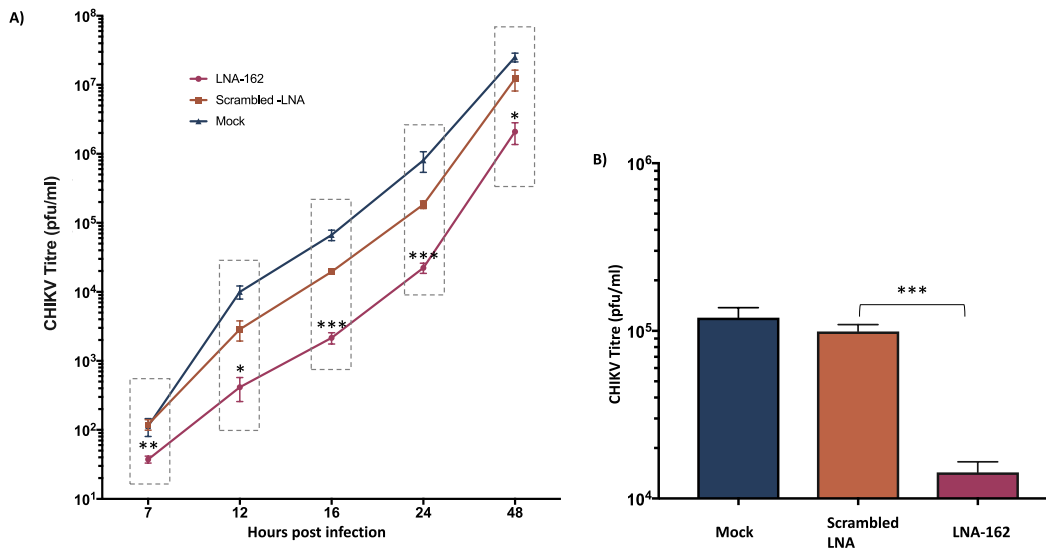


Fig. 5. A) CHIKV infection was inhibited at multiple time points for 48 hpi following LNA-162 transfection and B) pre-transfection with LNA-162 significantly inhibited productive infection. A) Analysis of productive CHIKV replication at 7, 12, 16, 24 and 48 hpi following transfection of 3000 nM LNA-162 or scrambled-LNA into Huh7 cells 3 hpi at an MOI of 1. Significant LNA-162 inhibition relative to scrambled control indicated by dashed grey boxes. B) Huh7 cells were transfected with LNA-162 or scrambled-LNA 4 h prior to CHIKV infection (MOI 10) and measurement of productive infection at 24 hpi. N = 3, error bars represent standard error from the mean and significance measured by two-tailed T-test for LNA-162 vs scrambled LNA (* = P < 0.05, ** = P < 0.01, *** = P < 0.001).

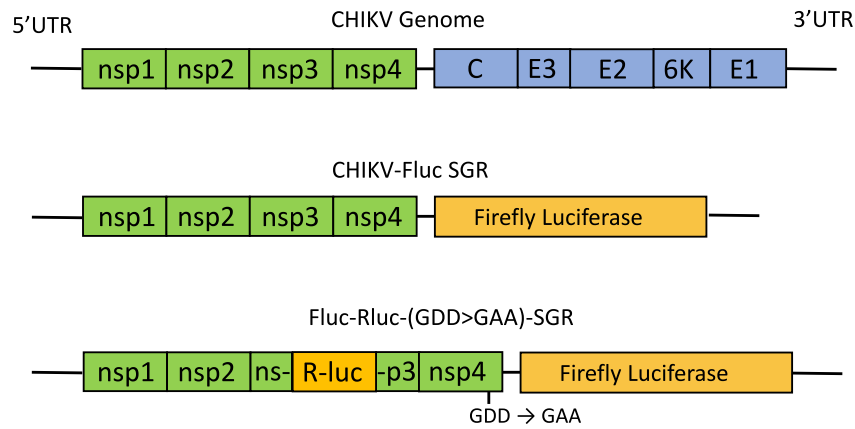


Fig. 6. Schematic representations of A) CHIKV genome, B) CHIKV-Fluc SGR and C) Fluc-Rluc-(GDD > GAA)-SGR. For Fluc-Rluc-(GDD > GAA)-SGR, a *Renilla* luciferase (R-luc) reporter is fused within the nsp3 coding sequence. The mutation GDD > GAA blocks nsp4 polymerase activity, allowing measurement of CHIKV ORF-1 translation independent of virus genome replication.

investigated the hypothesis that targeting these RNA structures with antisense LNAs would inhibit productive virus replication, through inhibition of CHIKV genome replication.

Alphavirus RNA is replicated in membrane bound replication complexes termed spherules and previous studies have indicated that replication complexes are most active in RNA synthesis at around 4 h.p.i (Pietilä et al., 2018), (Clewley and Kennedy, 1976; Pietilä et al., 2017a). LNA-162 was able to significantly inhibit CHIKV replication when transfected into infected cells at 3 h.p.i., indicating that the LNA is able to gain access to the viral RNA within the replication complex. Although CHIKV replication requires cellular chloride ion channels (Müller et al., 2019), these are likely not sufficient to transport oligonucleotide molecules. Since alphavirus RNA replication initially takes place at the plasma membrane (Frolova et al., 2010), it is possible that LNA-162 may bind prior to the formation of membrane-bound replication spherules. Alternatively, electron microscopy images of Sindbis virus infected BHK cells show that early replication complexes are connected to cytoplasmic side of the plasma membrane via a pore like structure (Jose et al., 2017),

through which LNAs could potentially enter the replication complexes from the cytoplasm. In addition to LNAs requiring entry into the replication complex, individual RREs may be unavailable for binding due to the presence of higher order RNA-RNA interactions or binding of *trans* activating factors, such as cellular or viral proteins. Our results indicate that SL165 is available for binding within the replication complex and that the hybridisation strength is likely sufficient to outcompete other RNA/RNA or RNA/protein interactions which could prevent LNA binding.

In order to confirm at which stage of the CHIKV replication LNA-162 was functioning, we utilised a sub-genomic replicon system, in which expression of firefly luciferase was used as a measure of genome replication. Inhibition of the sub-genomic replicon indicated that LNA-162 impairs CHIKV replication at the level of genome replication. We further confirmed that LNA-162 does not significantly impair translation of ORF-1, indicating that inhibition is due to LNA-162 acting directly on the viral RNA to prevent the function of the RRE SL165 during genome replication, rather than through steric hindrance of the translation

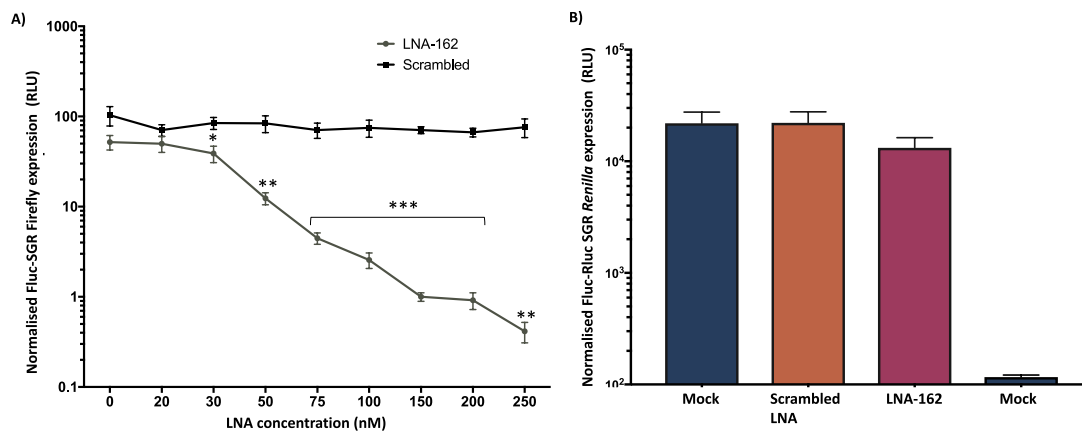


Fig. 7. LNA-162 inhibits CHIKV genome replication. A) LNA-162 inhibits CHIKV-Fluc SGR replication. Huh7 cells were co-transfected with CHIKV SGR and *Renilla* luciferase expressing transfection control RNA transcripts and either LNA-162 or scrambled-LNA at concentrations ranging from 1 to 250 nM. Luciferase expression was measured at 6 hpt and Firefly expressed relative to the *Renilla* luciferase transfection control. B) LNA-162 did not inhibit CHIKV-Rluc-(GDD-GAA)-SGR translation. Huh7 cells were co-transfected with CHIKV-Rluc-(GDD-GAA)-SGR and 100 nM of either LNA-162 or scrambled-LNA and *Renilla* luciferase measured at 6 hpt. N = 3, error bars represent standard error from the mean and significance measured by two-tailed T-test for LNA-162 vs scrambled LNA (* = $P \geq 0.04$, ** = $P \geq 0.01$, *** = $P \geq 0.001$).

machinery. Interestingly, LNA-202, (targeting CHIKV RRE SL194), was demonstrated to bind to the CHIKV genome by EMSA but did not inhibit either infectious CHIKV or replication of the sub-genomic CHIKV replicon (Supplementary Fig. 4). This suggests that not all CHIKV RREs are available for binding within the replication complex during active genome replication. Given that reverse genetic analysis previously demonstrated that SL194 is essential for efficient CHIKV genome replication in both mosquito and human cell lines, we hypothesise that these results indicate that binding of LNA-202 to SL194 within the replication complex is occluded, potentially by higher order RNA/RNA interactions or *trans* activating RNA binding proteins. It may also be possible that different anti-sense LNA oligonucleotides are variable in their ability to enter the replication complex or that LNA-202 does not have sufficient binding affinity to outcompete *trans* activating factors.

Since the first use of oligonucleotides to inhibit viral replication in the 1970s (Zamecnik and Stephenson, 1978), several antisense oligonucleotide drugs have been approved for use in a range of conditions. For example, Nusinersen is an antisense oligonucleotide used in treatment of spinal muscular atrophy (Bennett, 2019; Hua et al., 2008). In addition miravirsin, an LNA oligonucleotide treatment targeting host microRNA MiR-122, reached phase II clinical trials for in the treatment of HCV (Gebert et al., 2014). Although miravirsin did not enter the clinic, likely due to the development of direct acting antivirals (D'Ambrosio et al., 2017), this demonstrates the viability of the approach.

Viral RREs make attractive targets for novel anti-viral agents due to the essential roles which they play in viral replication and their specificity to the virus, which may limit off target side effects (Kendall et al., 2019). LNAs have previously been used to target RNA structures in a number of divergent RNA viruses. In HIV-1, LNAs have been used to block the dimerization initiation site, preventing formation of the genome homodimer (Elmén et al., 2004) and in HCV, LNAs targeting RNA stem-loop structures block interaction between the viral *cis*-acting replication element and the 3' non-coding region, causing inhibition of viral translation (Tuplin et al., 2015). Our data demonstrates that RREs in CHIKV can also be specifically targeted, suggesting that this approach can potentially be applied to many viruses which contain functional RREs.

In summary, for the first time we demonstrate that an RRE within the CHIKV genome can be specifically targeted using antisense LNA oligonucleotides, resulting in inhibition of productive virus replication by inhibition of CHIKV genome replication. We demonstrate that the viral replication complex is accessible to antisense LNAs and that the viral RRE SL165 is available for binding within the CHIKV replication

complex, whilst other RREs such as SL194 may be inaccessible. These findings further our understanding of CHIKV RNA replication and provide a rationale for the further development of antiviral agents targeting RREs within the CHIKV genome.

Funding

This work was supported by funding from the MRC to AT (MR/NO1054X/1) and BBSRC White Rose Doctoral Training Partnership [BB/M011151/1] to OP.

Declaration of competing interest

The authors declare that they have no known competing financial interests or personal relationships that could have appeared to influence the work reported in this paper.

Data availability

Data will be made available on request.

Appendix A. Supplementary data

Supplementary data to this article can be found online at <https://doi.org/10.1016/j.antiviral.2023.105523>.

References

- Bennett, C.F., 2019. Therapeutic antisense oligonucleotides are coming of age. *Annu. Rev. Med.* 70, 307–321.
- Burt, F.J., Chen, W., Miner, J.J., Lenschow, D.J., Merits, A., Schnettler, E., Kohl, A., Rudd, P.A., Taylor, A., Herrero, L.J., Zaid, A., Ng, L.F.P., Mahalingam, S., 2017. Chikungunya virus: an update on the biology and pathogenesis of this emerging pathogen. *Lancet Infect. Dis.* 17, e107–e117.
- Chery, J., Petri, A., Wagschal, A., Lim, S.-Y., Cunningham, J., Vasudevan, S., Kauppinen, S., Näär, A.M., 2018. Development of locked nucleic acid antisense oligonucleotides targeting Ebola viral proteins and host factor niemann-pick C1. *Nucleic Acid Therapeut.* 28, 273–284.
- Clewley, J.P., Kennedy, S.I.T., 1976. Purification and polypeptide composition of semliki forest virus RNA polymerase. *J. Gen. Virol.* 32, 395–411.
- D'Ambrosio, R., Degasperi, E., Colombo, M., Aghemo, A., 2017. Direct-acting antivirals: the endgame for hepatitis C? *Curr. Opin. Virol.*
- Dubey, S.K., Shrinet, J., Sunil, S., 2019. *Aedes aegypti* microRNA, miR-2944b-5p interacts with 3'UTR of chikungunya virus and cellular target vps-13 to regulate viral replication. *PLoS Neglected Trop. Dis.* 13, e0007429.
- Elmén, J., Zhang, H.-Y., Zuber, B., Ljungberg, K., Wahren, B., Wahlestedt, C., Liang, Z., 2004. Locked nucleic acid containing antisense oligonucleotides enhance inhibition

- of HIV-1 genome dimerization and inhibit virus replication. *FEBS Lett.* 578, 285–290.
- Fayzulini, R., Frolov, I., 2004. Changes of the secondary structure of the 5' end of the Sindbis virus genome inhibit virus growth in mosquito cells and lead to accumulation of adaptive mutations. *J. Virol.* 78, 4953–4964.
- Frolov, I., Hardy, R., Rice, C.M., 2001. Cis-acting RNA elements at the 5' end of Sindbis virus genome RNA regulate minus- and plus-strand RNA synthesis. *RNA* 7, 1638–1651.
- Frolova, E.I., Gorchakov, R., Pereboeva, L., Atasheva, S., Frolov, I., 2010. Functional Sindbis virus replicative complexes are formed at the plasma membrane. *J. Virol.* 84, 11679–11695.
- Ganesan, V.K., Duan, B., Reid, S.P., 2017. Chikungunya Virus: Pathophysiology, Mechanism, and Modeling. *Viruses* 9.
- Gebert, L.F.R., Rebhan, M.A.E., Crivelli, S.E.M., Denzler, R., Stoffel, M., Hall, J., 2014. Miravirsen (SPC3649) can inhibit the biogenesis of miR-122. *Nucleic Acids Res.* 42, 609–621.
- Gebhart, N.N., Sokolowski, K.J., Rupp, J.C., Hardy, R.W., 2015. Alphavirus RNA synthesis and non-structural protein functions. *J. Gen. Virol.* 96, 2483–2500.
- Gould, E.A., Gallian, P., de Lamballerie, X., Charrel, R.N., 2010. First cases of autochthonous dengue fever and chikungunya fever in France: from bad dream to reality. *Clin. Microbiol. Infect.* 16, 1702–1704.
- Grünweller, A., Hartmann, R.K., 2007. Locked nucleic acid oligonucleotides. *BioDrugs* 21, 235–243.
- Hua, Y., Vickers, T.A., Okunola, H.L., Bennett, C.F., Krainer, A.R., 2008. Antisense masking of an hnRNP A1/A2 intronic splicing silencer corrects SMN2 splicing in transgenic mice. *Am. J. Hum. Genet.* 82, 834–848.
- Jose, J., Taylor, A.B., Kuhn, R.J., 2017. Spatial and temporal analysis of alphavirus replication and assembly in mammalian and mosquito cells. *mBio* 8.
- Kendall, C., Khalid, H., Müller, M., Banda, D.H., Kohl, A., Merits, A., Stonehouse, N.J., Tuplin, A., 2019. Structural and phenotypic analysis of Chikungunya virus RNA replication elements. *Nucleic Acids Res.*
- Kendrick, K., Stanek, D., Blackmore, C., Centers for Disease Control and Prevention (CDC), 2014. Notes from the field: transmission of chikungunya virus in the continental United States—Florida, 2014. *MMWR Morb. Mortal. Wkly. Rep.* 63, 1137.
- Kulasegaran-Shylini, R., Atasheva, S., Gorenstein, D.G., Frolov, I., 2009. Structural and functional elements of the promoter encoded by the 5' untranslated region of the Venezuelan equine encephalitis virus genome. *J. Virol.* 83, 8327–8339.
- Kurreck, J., Wyszko, E., Gillen, C., Erdmann, V.A., 2002. Design of antisense oligonucleotides stabilized by locked nucleic acids. *Nucleic Acids Res.* 30, 1911–1918.
- Lemant, J., Boisson, V., Winer, A., Thibault, L., André, H., Tixier, F., Lemerrier, M., Antok, E., Cresta, M.P., Grivard, P., Besnard, M., Rollot, O., Favier, F., Huerre, M., Campinos, J.L., Michault, A., 2008. Serious acute chikungunya virus infection requiring intensive care during the reunion island outbreak in 2005–2006. *Crit. Care Med.* 36, 2536–2541.
- Li, X.-F., Jiang, T., Deng, Y.-Q., Zhao, H., Yu, X.-D., Ye, Q., Wang, H.-J., Zhu, S.-Y., Zhang, F.-C., Qin, E.-D., Qin, C.-F., 2012. Complete genome sequence of a chikungunya virus isolated in Guangdong, China. *J. Virol.* 86, 8904–8905.
- Marton, S., Berzal-Herranz, B., Garmendia, E., Cueto, F.J., Berzal-Herranz, A., 2012. Anti-HCV RNA aptamers targeting the genomic cis-acting replication element. *Pharmaceuticals* 5, 49–60.
- Mathur, K., Anand, A., Dubey, S.K., Sanan-Mishra, N., Bhatnagar, R.K., Sunil, S., 2016. Analysis of chikungunya virus proteins reveals that non-structural proteins nsP2 and nsP3 exhibit RNA interference (RNAi) suppressor activity. *Sci. Rep.* 6, 38065.
- Müller, M., Slivinski, N., Todd, E.J.A.A., Khalid, H., Li, R., Karwatka, M., Merits, A., Mankouri, J., Tuplin, A., 2019. Chikungunya virus requires cellular chloride channels for efficient genome replication. *PLoS Neglected Trop. Dis.* 13, e0007703.
- Niester, H.G., Strauss, J.H., 1990. Defined mutations in the 5' nontranslated sequence of Sindbis virus RNA. *J. Virol.* 64, 4162–4168.
- Oviedo-Pastrana, M., Méndez, N., Mattar, S., Arrieta, G., Gomezcaceres, L., 2017. Epidemic outbreak of Chikungunya in two neighboring towns in the Colombian Caribbean: a survival analysis. *Arch. Publ. Health* 75, 1.
- Pietilä, M.K., Albulescu, I.C., Hemert, M.J. van, Ahola, T., 2017a. Polyprotein processing as a determinant for in vitro activity of semliki forest virus replicase. *Viruses* 9, 292.
- Pietilä, M.K., Hellström, K., Ahola, T., 2017b. Alphavirus polymerase and RNA replication. *Virus Res.* 234, 44–57.
- Pietilä, M.K., van Hemert, M.J., Ahola, T., 2018. Purification of highly active alphavirus replication complexes demonstrates altered fractionation of multiple cellular membranes. *J. Virol.* 92.
- Pohjala, L., Utt, A., Varjak, M., Lulla, A., Merits, A., Ahola, T., Tammela, P., 2011. Inhibitors of alphavirus entry and replication identified with a stable chikungunya replicon cell line and virus-based assays. *PLoS One* 6, e28923.
- Pongsiri, P., Praianantathavorn, K., Theamboonlers, A., Payungporn, S., Poovorawan, Y., 2012. Multiplex real-time RT-PCR for detecting chikungunya virus and dengue virus. *Asian Pac. J. Trop. Med.* 5, 342–346.
- Rezza, G., Nicoletti, L., Angelini, R., Romi, R., Finarelli, A., Panning, M., Cordioli, P., Fortuna, C., Boros, S., Magurano, F., Silvi, G., Angelini, P., Dottori, M., Ciufolini, M., Majori, G., Cassone, A., CHIKV study group, 2007. Infection with chikungunya virus in Italy: an outbreak in a temperate region. *Lancet* 370, 1840–1846.
- Robinson, M.C., 1955. An epidemic of virus disease in Southern Province, Tanganyika territory, in 1952–1953. *Trans. R. Soc. Trop. Med. Hyg.* 49, 28–32.
- Schilte, C., Staikovsky, F., Couderc, T., Madec, Y., Carpentier, F., Kassab, S., Albert, M.L., Lecuit, M., Michault, A., Michault, A., 2013. Chikungunya virus-associated long-term arthralgia: a 36-month prospective longitudinal study. *PLoS Neglected Trop. Dis.* 7, e2137.
- Schwartz, O., Albert, M.L., 2010. Biology and pathogenesis of chikungunya virus. *Nat. Rev. Microbiol.* 8, 491–500.
- Solignat, M., Gay, B., Higgs, S., Briant, L., Devaux, C., 2009. Replication cycle of chikungunya: a re-emerging arbovirus. *Virology* 393, 183–197.
- Strauss, J.H., Strauss, E.G., 1994. The alphaviruses: gene expression, replication, and evolution. *Microbiol. Rev.* 58, 491–562.
- Suresh, G., Priyakumar, U.D., 2013. Structures, dynamics, and stabilities of fully modified locked nucleic acid (β -d-LNA and α -l-LNA) duplexes in comparison to pure DNA and RNA duplexes. *J. Phys. Chem. B* 117, 5556–5564.
- Tamberg, N., Lulla, V., Fragkoudis, R., Lulla, A., Fazakerley, J.K., Merits, A., 2007. Insertion of EGFP into the replicase gene of Semliki Forest virus results in a novel, genetically stable marker virus. *J. Gen. Virol.* 88, 1225–1230.
- Thaa, B., Biasiotto, R., Eng, K., Neuvonen, M., Götte, B., Rheinemann, L., Mutso, M., Utt, A., Varghese, F., Balistreri, G., Merits, A., Ahola, T., McInerney, G.M., 2015. Differential phosphatidylinositol-3-kinase-akt-mTOR activation by semliki forest and chikungunya viruses is dependent on nsP3 and connected to replication complex internalization. *J. Virol.* 89, 11420–11437.
- Titze-de-Almeida, R., David, C., Titze-de-Almeida, S.S., 2017. The race of 10 synthetic RNAi-based drugs to the pharmaceutical market. *Pharm. Res. (N. Y.)* 34, 1339–1363.
- Tsatsarkin, K.A., Vanlandingham, D.L., McGee, C.E., Higgs, S., 2007. A single mutation in chikungunya virus affects vector specificity and epidemic potential. *PLoS Pathog.* 3, e201.
- Tuplin, A., Struthers, M., Cook, J., Bentley, K., Evans, D.J., 2015. Inhibition of HCV translation by disrupting the structure and interactions of the viral CRE and 3' X-tail. *Nucleic Acids Res.* 43, 2914–2926.
- Van Bortel, W., Dorleans, F., Rosine, J., Blateau, A., Rousseau, D., Matheus, S., Leparc-Goffart, I., Flusin, O., Prat, C., Césaire, R., Najioullah, F., Ardillon, V., Balleydiere, E., Carvalho, L., Lemaître, A., Noël, H., Servas, V., Six, C., Zurbaran, M., Léon, L., Guinard, A., van den Kerkhof, J., Henry, M., Fanoy, E., Braks, M., Reimerink, J., Swaan, C., Georges, R., Brooks, L., Freedman, J., Sudre, B., Zeller, H., 2014. Chikungunya outbreak in the Caribbean region, december 2013 to march 2014, and the significance for Europe. *Euro Surveill.* 19, 20759.
- Weaver, S.C., Lecuit, M., 2015. Chikungunya virus and the global spread of a mosquito-borne disease. *N. Engl. J. Med.* 372, 1231–1239.
- Zamecnik, P.C., Stephenson, M.L., 1978. Inhibition of Rous sarcoma virus replication and cell transformation by a specific oligodeoxynucleotide. *Proc. Natl. Acad. Sci. U. S. A.* 75, 280–284.